

Hidden order in hexagonal $RMnO_3$ multiferroics ($R = Dy-Lu, In, Y,$ and Sc)

A. Cano*

CNRS, Université de Bordeaux, ICMCB, UPR 9048, F-33600 Pessac, France

(Received 2 December 2013; revised manuscript received 5 May 2014; published 17 June 2014)

Hexagonal $RMnO_3$ manganites are improper ferroelectrics in which the electric polarization is a by-product of the tripling of the unit cell. In $YMnO_3$, there is a second transition at ~ 920 K whose nature remains unexplained. We argue that this transition can be seen as a sort of hidden order in which a residual symmetry displayed by the trimerization order parameter is spontaneously broken. This additional order gives rise to 12 structural domains instead of six, and structural domain boundaries that can be either ferroelectric or nonferroelectric domain walls. We also suggest a generic $P6_3cm \leftrightarrow P3c1 \leftrightarrow P\bar{3}c1$ phase diagram, fully realized in $InMnO_3$.

DOI: [10.1103/PhysRevB.89.214107](https://doi.org/10.1103/PhysRevB.89.214107)

PACS number(s): 77.84.Bw, 77.80.-e, 61.50.Ah

Hexagonal $RMnO_3$ manganites, with $R = Dy-Lu, In, Y,$ and Sc , were discovered by Bertaut and collaborators half a century ago [1]. Nowadays, these compounds are considered as a distinguished class of multiferroic materials [2]. These systems are multiferroics for two reasons. On one hand, ferroelectricity appears at high temperature together with the tripling of the unit cell [3]. The interplay between the corresponding order parameters gives rise to remarkable features such as clamped ferroelectric-structural domain walls [4] with unusual transport properties [5]. On the other hand, antiferromagnetic order emerges at low temperatures [6], which fits out these systems with additional magnetoelectric properties [7].

$YMnO_3$ is probably the most studied member of this family. There is consensus that $YMnO_3$ is ferroelectric at room temperature, while it has a centrosymmetric structure above ~ 1250 K. The symmetry of the ferroelectric phase has been ascribed to the $P6_3cm$ space group. As such, it is connected to the high-temperature $P6_3/mmc$ structure by the tripling of the corresponding unit cell and the loss mirror symmetry perpendicular to the c axis. This is realized by the tilting and distortion of the MnO_5 bipyramids and the displacement of the Y atoms, which triggers the spontaneous electric polarization of the system (see Fig. 1). The exact nature of this ferroelectric transition, however, has been the subject of a debate that has intensified during the last decade [8–11].

At present, it is reasonably accepted that trimerization and polarization appear both at once. That is, the symmetry changes in one single step from $P6_3/mmc$ to $P6_3cm$ at 1250 K. Thus, the primary order parameter transforms according to the K_3 irreducible representation of the $P6_3/mmc$ space group, while the ferroelectricity is a by-product of the structural transition [10,11]. The system is therefore an improper ferroelectric [2,12]. Intriguingly, a second anomaly has been repeatedly reported around 920 K whose origin remains unclear [8,9]. The aim of this paper is to provide an explanation that is, in fact, generally valid for any improper ferroelectric and, in particular, for the hexagonal $RMnO_3$ manganites, suggesting a generic $P6_3cm \leftrightarrow P3c1 \leftrightarrow P\bar{3}c1$ phase diagram for these systems.

Conceptually, this type of secondary transition evokes the discussed by Levanyuk and Sannikov in the early days of

improper ferroelectrics [12,13]. Accordingly, it can be seen as a kind of residual symmetry breaking. The point is that the primary K_3 order parameter can generate different types of domains in which the symmetry can be broken at different levels. Specifically, the trimerization can be less symmetric than assumed so far (with electric dipoles neither totally compensated nor maximally uncompensated, but somewhere in between). The anomalies observed at ~ 920 K are likely related to the breaking of this residual symmetry. We note that the smoking gun for evidencing this phenomenon is not necessarily the electric polarization, as this observable displays only a part of the total symmetry that can actually be broken in the trimerization (i.e., via K_3).

In the case of $YMnO_3$, the initial expression of the free energy given by Fennie and Rabe [11] has been upgraded by Artyukhin *et al.* [14] by taking into account the actual two-component character of the corresponding order parameter $(\phi_1, \phi_2) = (\rho \cos \phi, \rho \sin \phi)$. This upgrade is essential, for example, for describing the topological defects that appear in these systems. The upgraded expression reads [15]

$$F = F_{\text{trim}} + F_P + F_{\text{int}}. \quad (1)$$

Here

$$F_{\text{trim}} = \frac{a}{2}\rho^2 + \frac{b}{4}\rho^4 + \frac{c}{6}\rho^6 + \frac{c'}{6}\rho^6 \cos 6\phi + \text{gradient terms}, \quad (2)$$

$$F_P = \frac{A}{2}P^2 + \text{gradient terms}, \quad (3)$$

represent independent contributions associated with the trimerization and the electric polarization, respectively, while

$$F_{\text{int}} = -gP\rho^3 \cos 3\phi + \frac{g'}{2}\rho^2 P^2 \quad (4)$$

describes the interplay between these variables. Furthermore, Artyukhin *et al.* obtained the parameters of this expression from *ab initio* calculations. Interestingly, the energetics of the trimerization is dominated by the interplay (4) as the bare anisotropy c' is positive and much weaker than the eventual anisotropy $\tilde{c}' = c' - \frac{3g^2}{2(a+g'\rho^2)} < 0$ obtained after minimization over P . The free energy (1) is illustrated in Fig. 2(a). It generates six different low-symmetry states characterized by the discrete values $\phi_n = n\pi/3$ ($n = 1, 2, \dots, 6$) for the phase

*cano@icmcb-bordeaux.cnrs.fr

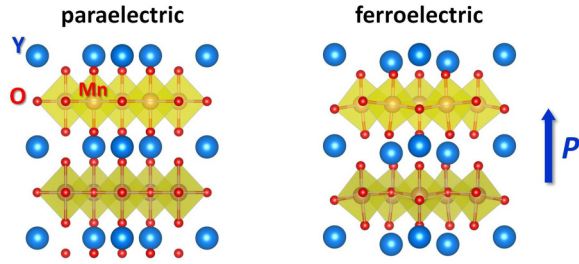


FIG. 1. (Color online) Atomic rearrangements associated with improper ferroelectricity in YMnO_3 , in which the spontaneous polarization P appears along the c axis.

of the trimerization order parameter. Since $P \sim \rho^3 \cos 3\phi$, there is a finite electric polarization associated with each of these domains that has equal magnitude for even and odd values of n but opposite signs.

In the following we extend this framework in order to reproduce the possibility of a second transition. We note that the above states minimize the free energy by providing the maximal reduction of the anisotropy term ($\cos 6\phi_n = 1$). Accordingly, these states can be seen as the most symmetric trimerization states that can be realized in the system. In particular, the new unit cell contains two unequal Y atoms according to their displacements along the c axis, while in general there can be three (see below). It thus exhibits a sort of accidental symmetry. No term in the free energy Eq. (1) penalizes this symmetry, which automatically excludes other types of solutions with further reduced symmetry. This contingent situation is actually unphysical according to that observed in Ref. [16] (see below). The simplest way to correct it is by supplementing (1) with the symmetry-allowed term

$$F' = \frac{f}{6} \rho^{12} \cos^4 3\phi. \quad (5)$$

If $f > 0$, the role of this term is to spoil the preference for symmetric solutions as the trimerization amplitude increases. Thus, the extended free energy eventually describes an additional phase in which the six initial domains are split into 12 different states. This is shown in Figs. 2(b) and 2(c). These domains can be characterized by the phases of the trimerization

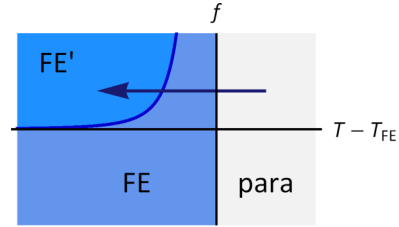


FIG. 3. (Color online) Schematic phase diagram for the model (1) and (5). As the temperature decreases, the paraelectric phase is replaced by a ferroelectric phase with residual symmetry that can be further broken if $f > 0$. The arrow indicates the path likely followed in YMnO_3 .

order parameter,

$$\phi_{n\pm} = \phi_n \pm \delta, \quad (6)$$

where δ is such that $\sin 3(\phi_n \pm \delta) = \pm(1 - \frac{|c'|}{f\rho^6})^{1/2}$. The resulting phase diagram is sketched in Fig. 3.

Similar to the sixth-order anisotropy term, Eq. (5) can have different origins. It can be due to the intrinsic anharmonicity of the K_3 phonons or due to their coupling to other variables. For instance, if the coefficient c' changes with P as $c' = c'_0 + c'_1 P^2$, then a term of the form (5) with $f \rightarrow 2c'_1 g^2/a^2$ is generated similarly to the sixth-order term obtained via the interaction (4). In principle, these terms can also be determined from first-principles calculations by extending the procedure reported in Ref. [14]. We emphasize that the Ginzburg-Landau theory constructed otherwise fails at reproducing all the possible ground-state symmetries that can actually be obtained via the primary K_3 order parameter. In this respect, such high-order functionals introduced by Levanyuk and Sannikov [12,13] have also been discussed in relation to the Higgs problem in high-energy physics [17], ferroelectric ferroelastics such as $\text{Tb}_2(\text{MoO}_4)_3$ [18], and, more recently, the magnetic phases of multiferroic CuO [19].

Alternatively, the secondary transition in YMnO_3 can be seen as driven by the additional order parameter Q that transforms according to the Γ_4^+ representation of the $P6_3/mmc$ space group—without the necessity of the term (5). At the lowest order in Q , the coupling between this variable

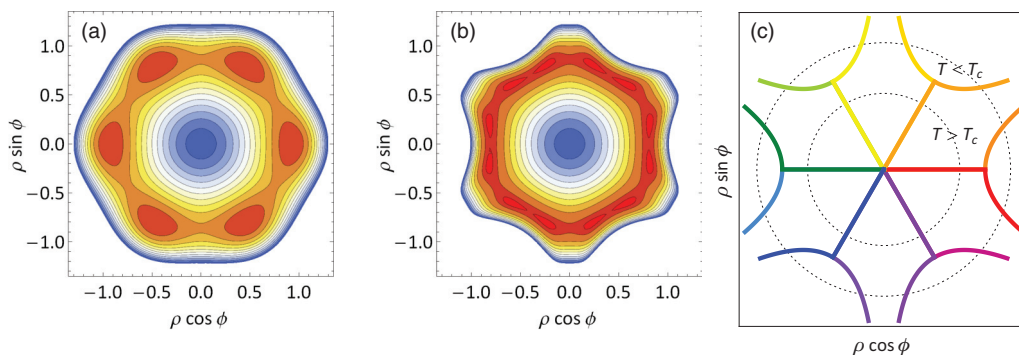


FIG. 2. (Color online) (a) Contour plot of the free energy (1). The parameters are taken from Ref. [14], which gives rise to six minima (in red). (b) The incorporation of the term (5) results in 12 minima ($f = 3 \text{ eV } \text{\AA}^{-12}$ for the sake of illustration). (c) Illustration of the transition from six to 12 domains as a function of the trimerization amplitude within the model (1) and (5). The lines represent the position of the different minima of the free energy. In all cases there are only two polarization domains since $P \sim \cos 3\phi$.

and trimerization order parameter is

$$F'_{\text{int}} = \lambda Q \rho^3 \sin 3\phi. \quad (7)$$

Thus, according to (1) and (7), the emergence of Q also implies the stabilization of additional trimerization states. In this case

$$\sin 3\phi_{n\pm} = -\lambda \frac{\tilde{c}}{\rho^6} Q, \quad (8)$$

where $Q \sim \pm|T - T_c|^{1/2}$ within the Ginzburg-Landau framework. From the point of view of symmetry, that obtained via the high-order term (5) is equivalent to this scenario. The physical interpretation, however, is rather different. In the first case, there is no need to invoke any additional order parameter, while the second possibility suggests that there is a sort of hidden Γ_4^+ order behind the second transition in the ferroelectric phase of YMnO_3 . We note that no Γ -point phonon corresponds to the Γ_4^+ symmetry in RMnO_3 [20]. Consequently, the Q variable itself is associated with orbital degrees of freedom rather than with atomic displacements. More microscopically, this scenario can therefore be linked to a charge ordering mechanism such as the one proposed by Khomskii and collaborators [21]. Experimentally, this can be verified by means of advanced synchrotron x-ray analyses [22] or scanning electron microscopies [23].

In both scenarios the additional transition implies a reduction of the nominal magnitude of the polarization since $|P| \sim |\cos 3\phi_{n\pm}| < 1$. This is in tune with experimental observations [9]. The fact that P eventually reaches a constant value can be understood as the saturation of both the trimerization order parameter and Q . The residual symmetry breaking describes a $P6_3cm$ to $P3c1$ transition in which both $P \sim \cos 3\phi$ and $Q \sim \sin 3\phi$ are nonzero. This is in fact the maximal symmetry breaking that can be obtained via the primary K_3 order parameter. It is worth noting that the x-ray diffraction patterns seem to be compatible with such maximally reduced symmetry [1,24,25]. We note that, in general, the temperature evolution can be such that P disappears completely even if the primary K_3 order parameter is nonzero. In that case, one recovers six structural domains but with a different $P\bar{3}c1$ space group symmetry. Interestingly, this would have been the case in YMnO_3 in the absence of the coupling (4) given that the bare anisotropy coefficient c' is positive, which favors $\sin 3\phi = \pm 1$ [14]. This possibility seems to be realized in InMnO_3 according to the first-principles calculations reported in Ref. [25]. It would be very interesting to study the effect of the (Y,In) substitution, as the complete sequence of $P6_3cm \leftrightarrow P3c1 \leftrightarrow P\bar{3}c1$ transitions between trimerized states could be realized as a function of this doping.

We have seen that the trimerization can give rise to six or 12 different structural domains, depending on whether or not a residual symmetry is preserved. In both cases nontrivial topological defects such as the vortex/antivortex pairs observed in Ref. [4] and the topological stripes discussed in Ref. [14] can be created. If the residual symmetry is preserved, the topological stability of these defects implies that the change in the trimerization angle across the domain walls is $\Delta\phi = \pm\pi/3$. However, if the residual symmetry is broken, these walls lose their topological stability and each of them will decay into a pair of different walls with $\Delta\phi = \pm(\pi/3 - 2\delta)$ and $\Delta\phi = \pm 2\delta$. We note that in both

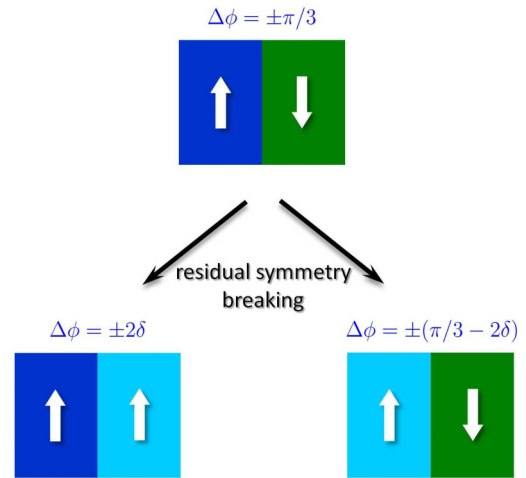


FIG. 4. (Color online) Structural domain boundaries expected in YMnO_3 . (a) If the residual symmetry of the primary K_3 order parameter is preserved, the change in the trimerization angle is $\Delta\phi = \pm\pi/3$ and structural and ferroelectric domain walls are interlocked. (b) If the residual symmetry is broken, the change in the trimerization angle can be either $\Delta\phi = \pm(\pi/3 - 2\delta)$ or $\Delta\phi = \pm 2\delta$, which generates ferroelectric and nonferroelectric domain walls, respectively. δ is determined by the amount of residual symmetry that is broken (either by the specific energetics of the trimerization or via a hidden Γ_4^+ order).

cases there are only two types of polarization domains. Thus, while in the first case the structural domain walls are also ferroelectric domain walls, in the second case we have both ferroelectric [$\Delta\phi = \pm(\pi/3 - 2\delta)$] and nonferroelectric domain walls ($\Delta\phi = \pm 2\delta$) (see Fig. 4). This implies that different C_6 and C_3 vortex/antivortex pairs, for example, can look the same if they are probed by means of a technique that reveals the electric polarization only. Nevertheless, these topological defects will interact differently with electric and strain fields, which can bring additional functionalities to the system. Specifically, ferroelectric domain walls are expected to react to the application of an electric field while the nonferroelectric ones are expected to remain passive. This can qualitatively modify the ferroelectric switching demonstrated in Ref. [26], for example. In the case of a topological vortex containing both walls, the motion of the ferroelectric walls will be stopped at the nonferroelectric ones since they cannot be annihilated due to the conservation of the corresponding topological charge. Thus, the eventual switching is expected to be controlled by both electrostatic and nonelectrostatic factors. As regards strains, they can also exert a force on this type of multiferroic walls due to the coupling $F_{\text{int}} = \lambda \rho^2 [(u_{xx} - u_{yy})\partial_x \phi - 2u_{xy}\partial_y \phi]$ [14,27]. Given a certain strain, this force basically depends on the variation of the trimerization angle at the domain wall. This variation is $\Delta\phi = \pm\pi/3$ if the residual symmetry is preserved, while it becomes $\Delta\phi = \pm(\pi/3 - 2\delta)$ and $\Delta\phi = \pm 2\delta$ if it is broken. Consequently, not only can the direction of the force change at different walls, but also its magnitude can be inherently different depending on whether or not the wall is ferroelectric. These types of long-range field-induced forces are known to be an important factor for the mutual interaction between topological defects [28]. Thus,

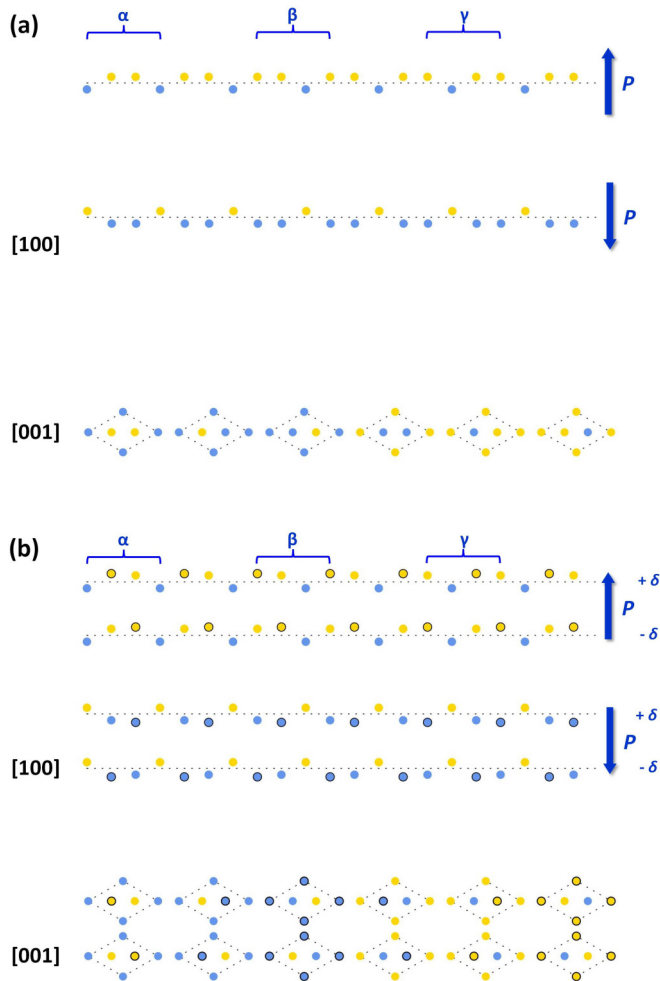


FIG. 5. (Color online) Schematic representation of the different ferroelectric R unit cells along the [001] and [100] directions. (a) The residual symmetry of the trimerization order parameter implies two types of R atoms according to their shift, upwards (yellow) or downwards (blue), with respect to their original positions in the paraelectric phase (along the dotted line). The origin of the unit cell determines the structural domains, frequently labeled as α_{\pm} , β_{\pm} , and γ_{\pm} (where \pm stands for the direction of the electric polarization). (b) The breaking of the residual symmetry generates three inequivalent R atoms, indicated by the additional circled symbols. The number of different unit cells becomes 12, and the corresponding domains could be labeled $\alpha_{\pm\pm}$, $\beta_{\pm\pm}$, and $\gamma_{\pm\pm}$, where the extra \pm stands for the deviation $\pm\delta$ of the trimerization angle from $n\pi/3$ ($n = 1, \dots, 6$) according to (6).

this interplay resulting from the residual symmetry breaking can substantially modify the Kibble-Zurek-like mechanisms proposed for their formation in $RMnO_3$ manganites [29].

Next, we discuss the atomic patterns associated with the different ferroelectric domains that can appear in $RMnO_3$. These are illustrated in Fig. 5. If the residual symmetry

is preserved, there are two types of R atoms within the [001] layers. The electric polarization is due to the relative displacement of these atoms along the c axis, which generates two ferroelectric domains. The structural domains, in their turn, are determined by the different origins of the unit cell. In contrast, if the residual symmetry is broken, the number of inequivalent R atoms becomes three. This increases the number of structural domains, while keeping the two possible directions for the electric polarization. We note that the atomic positions observed in Ref. [16] by means of scanning transmission electron microscopy (STEM) reproduce the second pattern, which confirms that the residual symmetry is broken in $YMnO_3$. More precisely, the STEM images reveal that the Y atoms are indeed placed at three different positions along the c axis. These positions are such that the sixfold symmetry axis of the supposed $P6_3cm$ structure is lost, while there is still a net polarization. This means that the actual symmetry of these domains is $P3c1$, as predicted in our model. We note also that similar STEM experiments in $InMnO_3$ have revealed $P\bar{3}c1$ domains, in which the displacements of the three nonequivalent In atoms compensate each other to produce a zero net polarization [30]. These domains eventually transform into $P6_3cm$ domains by lowering the temperature. Interestingly, this has been observed to occur via an “unusually sluggish transition.” We conjecture that this transition actually occurs via the $P3c1$ phase. This would be another confirmation of our model which, in contrast to previous proposals, naturally predicts such a $P6_3cm \leftrightarrow P3c1 \leftrightarrow P\bar{3}c1$ phase diagram.

In summary, we have pointed out that the secondary transition systematically observed in $YMnO_3$ is likely related to a residual symmetry breaking of the trimerization order parameter. This can be driven either by the specific energetics of the trimerization or by a hidden Γ_4^+ order. In both cases, 12 different structural domains are obtained out of the six initial states of the system, while the number of ferroelectric domains remains two. Thus, the structural domain boundaries can be either ferroelectric or nonferroelectric domain walls, which is expected to modify their interaction with the external fields. This enriches the physics of the topological defects characteristic of this type of multiferroics, which can reveal additional functionalities that deserve further studies. The proposed model is based on symmetry arguments and therefore valid for all the members of the hexagonal $RMnO_3$ family. Accordingly, a generic $P6_3cm \leftrightarrow P3c1 \leftrightarrow P\bar{3}c1$ phase diagram is proposed for these systems. We have argued that, in addition to the secondary transition in $YMnO_3$, the unusual sluggishness of the paraelectric-ferroelectric transition observed in $InMnO_3$ is due to the emergence of the additional $P3c1$ phase displaying full symmetry breaking. Our work emphasizes that, more than 50 years after their discovery, hexagonal $RMnO_3$ manganites keep showing unique physics and therefore is expected to motivate future studies.

I thank A. Levanyuk, D. Meier, and M. Pollet for useful discussions, and S.-W. Cheong for pointing me to Ref. [30].

[1] H. L. Yakel, W. C. Koehler, E. F. Bertaut, and E. F. Forrat, *Acta Crystallogr.* **16**, 957 (1963).

[2] M. Fiebig, *J. Phys. D* **38**, R123 (2005); S.-W. Cheong and M. Mostovoy, *Nat. Mater.* **6**, 13 (2007).

- [3] E. F. Bertaut, F. Forrat, and P. H. Fang, *C. R. Acad. Sci.* **256**, 1958 (1963).
- [4] T. Choi, Y. Horibe, H. T. Yi, Y. J. Choi, W. Wu, and S.-W. Cheong, *Nat. Mater.* **9**, 253 (2010).
- [5] D. Meier, S. Seidel, A. Cano, K. Delaney, Y. Kumagai, M. Mostovoy, N. A. Spaldin, R. Ramesh, and M. Fiebig, *Nat. Mater.* **11**, 284 (2012).
- [6] E. F. Bertaut and M. Mercier, *Phys. Lett.* **5**, 27 (1963).
- [7] M. Fiebig, Th. Lottermoser, D. Frohlich, A. V. Goltsev, and R. V. Pisarev, *Nature (London)* **419**, 818 (2002); Th. Lottermoser, Th. Lonkai, U. Amann, D. Hohlwein, J. Ihringer, and M. Fiebig, *ibid.* **430**, 541 (2004); S. Petit, F. Moussa, M. Hennion, S. Pailhes, L. Pinsard-Gaudart, and A. Ivanov, *Phys. Rev. Lett.* **99**, 266604 (2007); S. Lee, A. Pirogov, M. Kang, K.-H. Jang, M. Yonemura, T. Kamiyama, S.-W. Cheong, F. Gozzo, N. Shin, H. Kimura, Y. Noda, and J.-G. Park, *Nature (London)* **451**, 805 (2008).
- [8] See, e.g., I. G. Ismailzade and S. A. Kizhaev, *Fiz. Tverd. Tela* **7**, 298 (1965) [*Solid State Phys.* **7**, 236 (1965)]; T. Katsufuji, S. Mori, M. Masaki, Y. Moritomo, N. Yamamoto, and H. Takagi, *Phys. Rev. B* **64**, 104419 (2001); T. Katsufuji, M. Masaki, A. Machida, M. Moritomo, K. Kato, E. Nishibori, M. Takata, M. Sakata, K. Ohoyama, K. Kitazawa, and H. Takagi, *ibid.* **66**, 134434 (2002); B. B. van Aken, T. T. M. Palstra, A. Filippetti, and N. A. Spaldin, *Nat. Mater.* **3**, 164 (2004); G. Nénert, Y. Ren, H. T. Stokes, and T. T. M. Palstra, [arXiv:cond-mat/0504546](https://arxiv.org/abs/cond-mat/0504546); G. Nénert, M. Pollet, S. Marinell, G. R. Blake, A. Meetsma, and T. T. M. Palstra, *J. Phys.: Condens. Matter* **19**, 466212 (2007); J. Kim, K. C. Cho, Y. M. Koo, K. P. Hong, and N. Shin, *Appl. Phys. Lett.* **95**, 132901 (2009); J. Kim, Y. M. Koo, K.-S. Sohn, and N. Shin, *ibid.* **97**, 092902 (2010).
- [9] A. S. Gibbs, K. S. Knight, and P. Lightfoot, *Phys. Rev. B* **83**, 094111 (2011).
- [10] T. Lonkai, D. G. Tomuta, U. Amann, J. Ihringer, R. W. Hendriks, D. M. Tobbens, and J. A. Mydosh, *Phys. Rev. B* **69**, 134108 (2004).
- [11] C. J. Fennie and K. M. Rabe, *Phys. Rev. B* **72**, 100103 (2005).
- [12] A. P. Levanyuk and D. G. Sannikov, *Sov. Phys. Usp.* **17**, 199 (1974).
- [13] A. P. Levanyuk and D. G. Sannikov, *JETP Lett.* **11**, 43 (1970); *Sov. Phys. JETP* **33**, 600 (1971).
- [14] S. Artyukhin, K. T. Delaney, N. A. Spaldin, and M. Mostovoy, *Nat. Mater.* **13**, 42 (2014).
- [15] It can be seen that, even if we are dealing with rather high transition temperatures, our mean-field approach is justified. The Ginzburg-Levanyuk criterion defines the region in which this approach is overwhelmed by critical fluctuations [see, e.g., L. D. Landau and E. M. Lifshitz, *Statistical Physics* (Elsevier, Amsterdam, 1980), Part 1, Sec. 146]. In the case of a two-component order parameter such as YMnO₃, this criterion can be deduced as explained by A. Larkin and A. Varlamov, in *Handbook on Superconductivity: Conventional and Unconventional Superconductors*, edited by K.-H. Bennemann and J. B. Ketterson (Springer, Berlin, 2002). Thus, in terms of the parameters of Eq. (1), the Ginzburg-Levanyuk number reads $G_i = \frac{b^2 d^6}{(4\pi)^2 \alpha s^3} T_c$, where $\alpha = |a_{T=0}|/T_c$, s is the gradient stiffness, and d is the characteristic length associated with the trimerization order parameter (~ 1 Å according to Refs. [11, 14]). Despite the fact that the temperature dependence of these parameters is certainly oversimplified, the values calculated in Ref. [14] allow to reproduce well key quantities such as the ferroelectric polarization up to remarkably high temperatures. These values then can be safely used to estimate the Ginzburg-Levanyuk number. The result is $G_i \sim 3 \times 10^{-7}$, which signals that critical fluctuations are unimportant for our purposes (as they can hardly explain the presence of a secondary anomaly which is ~ 300 K below the T_c). On top of that, there are obviously local Debye-Waller-factor-like fluctuations. These, however, are associated with the the melting transition rather than to the transitions of our interest.
- [16] Q. Zhang, G. Tan, L. Gu, Y. Yao, Ch. Jin, Y. Wang, X. Duan, and R. Yu, *Sci. Rep.* **3**, 2741 (2013).
- [17] J. S. Kim, *Nucl. Phys. B* **207**, 374 (1982).
- [18] S. Galam and J. L. Birman, *Phys. Rev. Lett.* **51**, 1066 (1983).
- [19] P. Toledano, N. Leo, D. D. Khalyavin, L. C. Chapon, T. Hoffmann, D. Meier, and M. Fiebig, *Phys. Rev. Lett.* **106**, 257601 (2011).
- [20] M. N. Iliev, H. G. Lee, V. N. Popov, M. V. Abrashev, A. Hamed, R. L. Meng, and C. W. Chu, *Phys. Rev. B* **56**, 2488 (1997); J. Varignon, S. Petit, and M.-B. Lepetit, [arXiv:1203.1752](https://arxiv.org/abs/1203.1752).
- [21] D. V. Efremov, J. van der Brink, and D. I. Khomskii, *Nat. Mater.* **3**, 853 (2004).
- [22] M. S. Senn, J. P. Wright, and J. P. Attfield, *Nature (London)* **481**, 173 (2012); S. Mondal, S. van Smaalen, G. Parakhonskiy, S. J. Prathapa, L. Noohinejad, E. Bykova, N. Dubrovinskaya, D. Chernyshov, and L. Dubrovinsky, *Phys. Rev. B* **88**, 024118 (2013).
- [23] H. Tan, S. Turner, E. Yucelen, J. Verbeeck, and G. Van Tendeloo, *Phys. Rev. Lett.* **107**, 107602 (2011).
- [24] D. A. Rusakov, A. A. Belik, S. Kamba, M. Savinov, D. Nuzhnyy, T. Kolodiazhnyi, K. Yamaura, E. Takayama-Muromachi, F. Borodavka, and J. Kroupa, *Inorg. Chem.* **50**, 3559 (2011).
- [25] Y. Kumagai, A. A. Belik, M. Lilienblum, N. Leo, M. Fiebig, and N. A. Spaldin, *Phys. Rev. B* **85**, 174422 (2012).
- [26] M.-G. Han, Y. Zhu, L. Wu, T. Aoki, V. Volkov, X. Wang, S. Chul Chae, Y. S. Oh, and S.-W. Cheong, *Adv. Mater.* **25**, 2415 (2013).
- [27] X. Wang, M. Mostovoy, M. G. Han, Y. Horibe, T. Aoki, Y. Zhu, and S.-W. Cheong, *Phys. Rev. Lett.* (to be published).
- [28] J. Lajzerowicz and A.P. Levanyuk, *Phys. Rev. B* **49**, 15475 (1994); A. P. Levanyuk, S. A. Minyukov, and A. Cano, *ibid.* **66**, 014111 (2002); A. Cano, A. P. Levanyuk, and S. A. Minyukov, *ibid.* **68**, 144515 (2003).
- [29] S. C. Chae, N. Lee, Y. Horibe, M. Tanimura, S. Mori, B. Gao, S. Carr, and S. W. Cheong, *Phys. Rev. Lett.* **108**, 167603 (2012); S. M. Griffin, M. Lilienblum, K. T. Delaney, Y. Kumagai, M. Fiebig, and N. A. Spaldin, *Phys. Rev. X* **2**, 041022 (2012).
- [30] F.-T. Huang, X. Wang, Y. S. Oh, K. Kurushima, S. Mori, Y. Horibe, and S.-W. Cheong, *Phys. Rev. B* **87**, 184109 (2013).